Self-Adapting Under-Ice Integrated Communications and Navigation Network

Toby Schneider
GobySoft, LLC
Mashpee, MA, USA
toby@gobysoft.org

Henrik Schmidt* and Supun Randeni†
Department of Mechanical Engineering
Massachusetts Institute of Technology
Cambridge, MA, USA
*henrik@mit.edu, †supun@mit.edu

***Abstract*—Complex vehicle missions (such as under-ice operations) require balancing the various competing uses of the acoustic channel. We present an integrated communications and navigation system, where a single synchronized digital communication packet is used to both provide tracking and data to the operator. In response, a navigation correction is telemetered to the vehicle. This system was deployed and operating during the ICEX20 experiment in the Beaufort Sea in March 2020.**

The variability of acoustic propagation with depth in the Beaufort Sea imposes a challenge to ensure reliable connectivity between the vehicle and the topside operators (in this case, via ice buoys). In the context of this under-ice system, where the ice buoys have multiple receiver and transmitter depths, we explore a self-adapting network that uses oceanographic and propagation modeling to predict the expected optimal receiver depth layer and transmitter hydrophone.

***Index Terms*—acoustic communication, undersea networking, virtual ocean, self-adapting networks**

I. Introduction

A. Simultaneous navigation and communications

Acoustic bandwidth is a finite resource for the competing needs of underwater vehicle operations: sensing, digital communications, and navigation subsystems all compete for a slice of time and frequency. As missions become more complex and risky, such as the under-ice operations in the Beaufort Sea that form the motivation for this paper, the need to de-conflict these various uses of the acoustic channel grows.

In this Integrated Communications and Navigation Networking (ICNN) system, a single synchronized digital communication packet is sent by the vehicle to several ice buoys. This signal is simultaneously used to carry information and to provide a time-of-flight trilateration fix for the vehicle's position. This fix is then transmitted down to the vehicle as a correction to the vehicle's navigation solution. The resulting hybrid communications/navigation system (described in Section II) is analogous to traditional long baseline (LBL) navigation (but where vehicle tracking is available topside) coupled with acoustic communications.

B. Self-adapting receiver and transmit selection

The Beaufort Sea has undergone significant changes in recent years due to global warming effects [1]–[3]. Here, the main feature of interest is the Beaufort Lens, a warm water layer that causes a double duct in the sound speed profile and disrupts the historically monotonically increasing sound speed with depth (see Fig. 1). The resulting shadow zone, as shown in [4], means that a single receiver at one depth can no longer provide good connectivity to a vehicle operating over a wide range of depths. In response, we designed a system with ice buoys that has receivers at two distinct depths: around 30 meters (to provide coverage in the upper channel) and around 90 meters (to provide coverage in the lower channel).

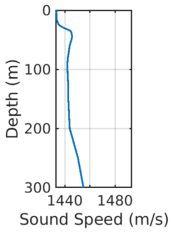

Fig. 1: Typical ICEX20 Sound speed profile with Beaufort lens at around 40 m depth

Given this choice of receiver depths, we developed a system based on prior work in the Virtual Ocean physics-based environmental modeling infrastructure [5] combined with acoustic propagation modeling to provide a prediction of the best depth to receive transmissions from the vehicle, and the preferred transducer (which buoy and at which depth) from which to send telemetry back to the vehicle. This system self-adapts with each update of the vehicle's position and depth based on the modeled propagation and several predicted performance metrics, described in Section III.

C. Prior work

We have shown vehicle adaptivity with depth [6] for missions that are not particular to a given operating depth. The buoy selection in this paper can be thought of the inverse problem: the vehicle depth is fixed due to the mission requirements but the buoy receiver depths can change.

Using synchonized acoustic communications transmissions for vehicle navigation has been explored for some time in more benign environments [7], [8]. Use of traditional long-base line navigation on the Arctic ice cover for AUV operations

Work supported by the Office of Naval Research, Code 322OA

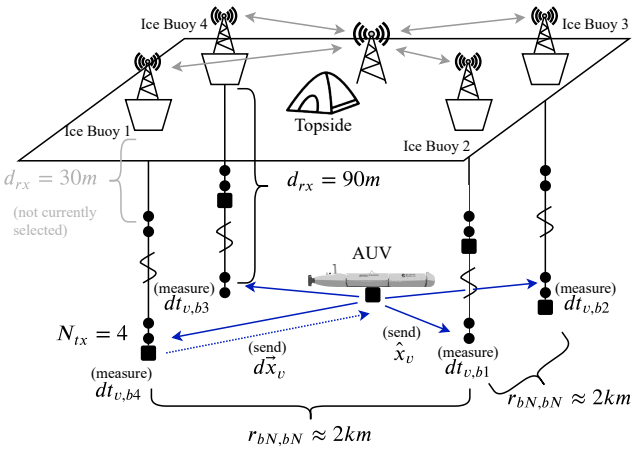

Fig. 2: Sketch of the ICNN as deployed in ICEX20. Ranges between buoys ($r_{bN,bN}$) can vary due to ice motion and are measured continuously using GPS. In this sketch, the Optimizer code has selected the deeper (90m) layer for receive (receiver hydrophones shown as circles) and buoy 4 ($N_{tx} = 4$) for transmit (transmitter transducers are shown as squares).

is discussed in [9], where the authors especially note the difficulty of accurately estimating the group velocity used for turning travel time into ranges.

The authors of [10] also explore a system where a single communications packet is used to improve navigation. This work is based on a "pseudorange" estimate derived from phase tracking over the duration of the communications signal. Such a technique could be complementary to the work presented here, especially for longer duration, lower frequency communications packets.

II. Integrated Communications and Navigation

The goal of this system was to provide acoustic data telemetry and global navigation corrections for one or more autonomous underwater vehicles (AUVs) operating under the Arctic ice cover in the Beaufort Sea. This was implemented (see Fig. 2) using the WHOI Micro-Modem [11] (10kHz carrier, 5kHz bandwidth, phase-shift keying (PSK) modulation) on four ice buoys. These modems were outfitted with a four-element receiver array, with two elements above the Beaufort Lens at 30 meters ("shallow layer"), and two elements below at 90 meters ("deep layer"). In addition, each modem had a transmitter transducer at one of the two depths, such that half of the buoys could transmit in the deep layer and half in the shallow. The buoys were connected wirelessly via radio to the topside base station, and were outfitted with a GPS to provide time synchronization and position. The choice of four buoys was made to provide an unambiguous planar trilateration solution with one additional buoy as spare and decreased uncertainty when all four were functional.

The AUV was also outfitted with a 10 kHz WHOI Micro-Modem. During operations, the vehicle transmitted datagrams (see Fig. 3) precisely on the second as synchronized by an

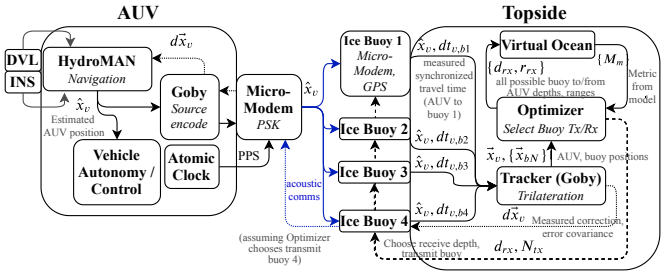

Fig. 3: Diagram of the data flow between the AUV and topside components (simplified to relevant components) in the ICNN system. A time-synchonized navigation estimate is regularly sent from HydroMAN on the AUV to up to four buoys, where a correction is computed in the Tracker and re-sent to the AUV. In parallel, the best receiver layer and transmitter hydrophone are selected by a Virtual Ocean model-driven Optimizer process.

on-board Microsemi Chip Scale Atomic Clock (CSAC). Each datagram contained the vehicle's navigation solution ($\hat{x}_v$) as estimated by the navigation subsystem ("HydroMAN"), along with other mission data prioritized by Goby-Queue [12] for a total of up to 64 bytes payload and was source encoded by the Dynamic Compact Control Language (DCCL) [13].

Upon receipt of this datagram by one or more ice buoys, they provided the calculated time-of-flight ($dt_{v,bN}$ for buoy N) based on the packet detection time, along with the buoy's GPS position and contents of the datagram to topside. Given the travel times from two buoys, the vehicle position ($\vec{x}_v$) and uncertainty covariance were computed immediately using least squares trilateration (with the aid of $\hat{x}_v$ to break ambiguity). When packets arrived at a (possible) third and fourth buoy, the solution was recalculated providing a new best solution. In each case, the Virtual Ocean model [5] was used to estimate the group velocity for each transmission path, providing a reliable and accurate method for converting travel time to range, overcoming the velocity estimation problem in [9].

After a configurable time, the topside transmitted the best available trilateration solution as a correction $d\vec{x}_v$ where

$$d\vec{x}_v = \vec{x}_v - \hat{x}_v \tag{1}$$

as the correction has higher information entropy than a global (latitude/longitude) position. This datagram (also including any additional commands) was sent to the vehicle using one of the buoys (see Section III for more on this selection). Upon receipt, the HydroMAN navigation would correct the time-lag of $d\vec{x}_v$ using a vehicle dynamic model and update the navigation filter along with an ice drift estimate as shown in Fig. 3. The ice drift estimate used to correct the DVL velocities was provided to the vehicle from the topside's filtered GPS. This drift can be significant depending on weather and ice motion, though it was less than 0.04 m/s for the calm weather during the operations presented here.

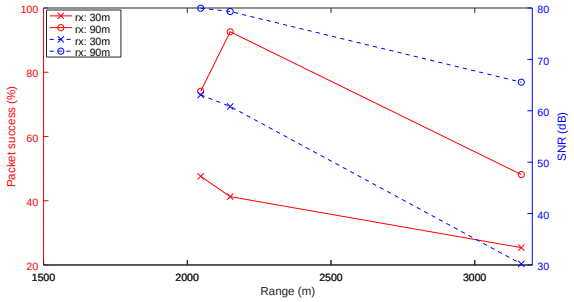

(a) $d_{tx} = 90m$ for SNR metric

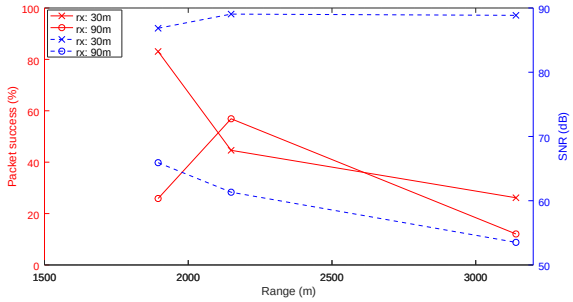

(b) $d_{tx} = 30m$ for SNR metric

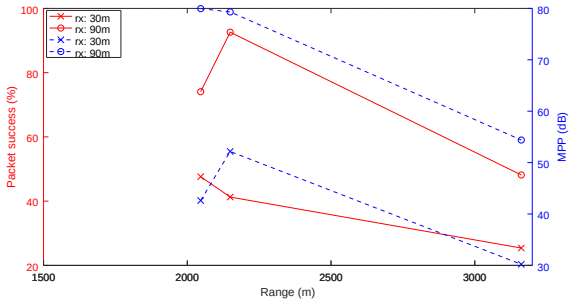

(c) $d_{tx} = 90m$ for MPP metric

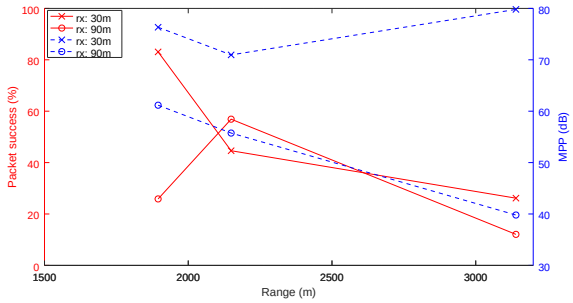

(d) $d_{tx} = 30m$ for MPP metric

Fig. 4: Measured packet success (red solid line) for deep transmitter (left) compared with prediction (blue dashed line) metrics and packet success for shallow transmitter (right). For the MPP metric, $\tau = 20ms$, and p = 3.

III. Automatic Selection of Ice Buoy Transmitter and Receivers

On the topside, the modeled propagation between the vehicle and all the receiver hydrophones of the ice buoys was continually calculated using each vehicle position ($\vec{x}_v$) from the Tracker, and the GPS position of each buoy ($\vec{x}_{bN}$), as shown in Fig. 3.

This modeled propagation for each possible path was used to compute several predicted performance metrics based on realtime ray tracing in the Virtual Ocean ($\{M_m\}$): (analog) signal-to-noise ratio (SNR) and SNR with multipath penalty (MPP). SNR is defined as usual as:

$$SNR = SL - NL - TL \tag{2}$$

The MPP metric penalizes multipath (which tends to lead to intersymbol interference) by reducing the effective power (using multipath loss MPL) of closely spaced ray paths in computing the received signal strength:

$$MPP = SL - NL - TL - MPL \tag{3}$$

$$MPL = -10 * log_{10}\left(1 - \frac{P_{mpp}}{P_{max}}\right)^{p} \tag{4}$$

where P_{mpp} is the power of the second strongest ray that arrives less than τ seconds before or after another ray, P_{max} is the power of the strongest ray, and p is a penalty factor (where larger p penalizes multiple arrivals more).

Given this information, the Optimizer chooses the given receiver layer which maximizes the chosen metric for any three buoys (the minimum for an unambiguous trilateration solution). This selection occurs after each update of the vehicle's position.

In addition to choosing the receiver layer, the Optimizer also chooses the transmitter buoy (N_{tx}) that would maximize the chosen metric for the modeled propagation path from this transmitter to the AUV.

IV. Results

The ICEX20 experiment was conducted from March 7 through March 11, 2020 on an ice camp in the Beaufort Sea around 71.17733°N, 142.40424°W. The results presented here are from a fixed transmission experiment using the buoys to simulate various static vehicle locations on March 10, 2020, and during about 11 km of untethered AUV runs at various ranges and depths during March 11, 2020.

A. Fixed Transmitter results

During actual vehicle operations, the ICNN was run to maximize communications performance for vehicle safety and vehicle mission data transfer. These runs did not provide statistics for comparing performance of the tracking range at different receive depths.

Thus, while the AUV was not in the water, we performed a series of experiments where one buoy at a time was chosen to simulate the AUV position (at the fixed range and depth which the buoy tranmitter transducer was deployed), and transmit regularly while receiving on the other buoys using the shallow

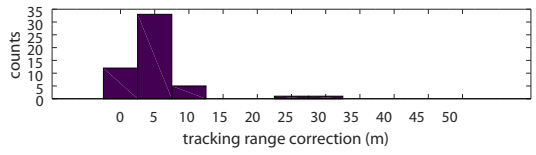

(a) Fixed transmitter (Buoy 1)

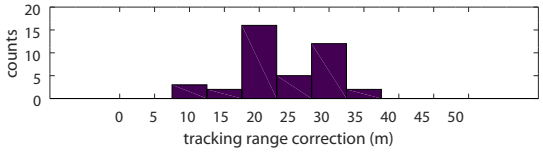

(b) Fixed transmitter (Buoy 2)

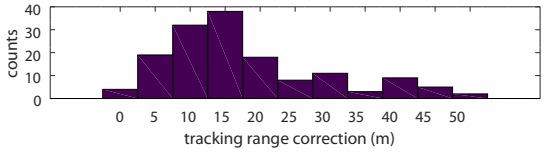

(c) AUV Untethered run

Fig. 5: Fig. 5a and 5b give the ICNN corrections to a GPS derived position and thus represent the tracking range error. In Fig. 5c, these corrections were applied to the vehicle estimated navigation from the HydroMAN system (which includes the DVL, INS, dynamic model, the ICNN), which means errors from both navigation and the tracking range are contained in these results. Occasional outliers (caused by bottom bounces or hardware timing issues) are not shown as they were rejected by HydroMAN. The delay between corrections was 47.9 seconds on average (minimum: 28 seconds, maximum: 150 seconds).

hydrophones. Then, the same buoy was used to transmit (again as if it were the vehicle) while receiving on the other buoys using the deep hydrophones. Fig. 4 shows the results of two of these locations; in Figs. 4a and 4c, buoy 1 (deep transmitter) was used to mimic the AUV, and in Figs. 4b and 4d, buoy 2 (shallow transmitter) was used as the AUV. The actual percentage of packets received is shown, compared with the model driven performance metrics. In most of the ranges tested, all of the metrics would choose the receiver layer which provided the higher overall chance of packet success. The one exception is the receiver at 2.1 km from the shallow transmitter (buoy 1) where the deep receiver performed slightly better than the shallow receiver. This exposes the difficulty of accurately predicting modem perfomance in the field, where variations in deployment procedure, hardware irregularities, and uncaptured environmental variation all play a role in overall performance.

B. Untethered AUV runs

On March 11, 2020, we performed a variety of different tethered and untethered vehicle missions, the latter of which were used for the figures presented here. The untethered operations covered about 11 km and covered ranges from the buoys between 1 km to 4 km. As shown in Fig. 5, the tracking range was able to provide navigation accuracies in the low

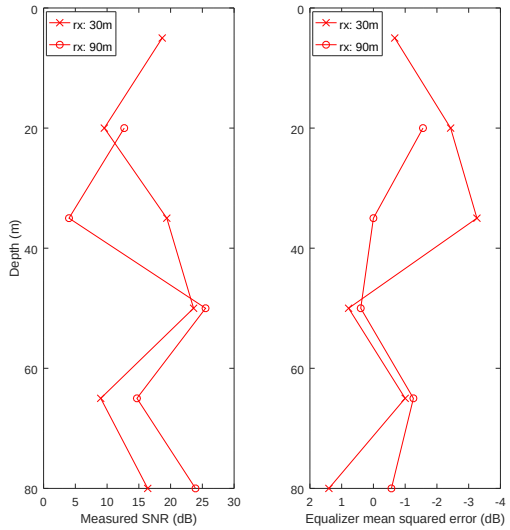

Fig. 6: Micro-Modem measured performance values over vehicle depth for the shallow and deep receive layers, showing that typically the shallow receivers perform better for a shallow transmitter and deeper receivers for a deeper transmitter.

tens of meters, on the same order of magnitude as GPS in the high latitudes. During operations, the Virtual Ocean model was regularly updated (at least daily) by sound speed profile data from CTD casts.

Fig. 6 shows the reported performance values (SNR and equalizer mean squared error) as a function of depth, averaged over all the ranges of the vehicle. This shows a general relationship between improved performance using the shallow receivers for shallow transmit depths, and deeper receivers for deeper transmit depths.

V. Conclusion

This experiment demonstrates the value of a hybrid communications and tracking system for providing both reliable bi-directional communications and navigation corrections for under-ice AUV operations. In addition, it demonstrates the feasibility of using model-based prediction for choosing between receiver depths to increase modem performance.

However, it also shows the difficulty in accurately predicting modem performance using models alone. As an extension to this work, future investigations may find that adding a machine learning approach based on observed data will improve performance, especially in longer running missions where collecting sufficient training data is feasible.

Acknowledgment

We greatly appreciate the help of Dennis Giaya, Lee Freitag, and the team in the Micro-Modem group at the Woods Hole Oceanographic Institution for their excellent support.

Also, many thanks to the Arctic Submarine Lab, UIC Science, and the rest of the ICEX20 team for making this experiment possible.

REFERENCES

[1] K. R. Wood, J. E. Overland, S. A. Salo, N. A. Bond, W. J. Williams, and X. Dong, "Is there a new normal climate in the beaufort sea?" *Polar Research*, vol. 32, no. 1, p. 19552, 2013.

[2] L. Freitag, K. Ball, J. Partan, P. Koski, and S. Singh, "Long range acoustic communications and navigation in the arctic," in *OCEANS'15 MTS/IEEE Washington*. IEEE, 2015, pp. 1–5.

[3] A. B. Baggeroer, H. Schmidt, S. A. Carper, J. Collis, and J. Rosenthal, "Detection and communication in the beaufort lens," *The Journal of the Acoustical Society of America*, vol. 140, no. 4, pp. 3408–3408, 2016.

[4] H. Schmidt and T. Schneider, "Acoustic communication and navigation in the new arctic - a model case for environmental adaptation," in *Underwater Communications and Networking Conference (UComms), 2016 IEEE Third*. IEEE, 2016, pp. 1–4.

[5] T. Schneider and H. Schmidt, "Netsim: A realtime virtual ocean hardware-in-the-loop acoustic modem network simulator," in *2018 Fourth Underwater Communications and Networking Conference (UComms)*. IEEE, 2018, pp. 1–5.

[6] ——, "Model-based adaptive behavior framework for optimal acoustic communication and sensing by marine robots," *IEEE Journal of Oceanic Engineering*, vol. 38, no. 3, pp. 522–533, July 2013.

[7] R. M. Eustice, L. L. Whitcomb, H. Singh, and M. Grund, "Experimental results in synchronous-clock one-way-travel-time acoustic navigation for autonomous underwater vehicles," in *Proceedings 2007 IEEE International Conference on Robotics and Automation*. IEEE, 2007, pp. 4257–4264.

[8] S. E. Webster, R. M. Eustice, H. Singh, and L. L. Whitcomb, "Preliminary deep water results in single-beacon one-way-travel-time acoustic navigation for underwater vehicles," in *2009 IEEE/RSJ International Conference on Intelligent Robots and Systems*. IEEE, 2009, pp. 2053–2060.

[9] C. Kunz, C. Murphy, R. Camilli, H. Singh, J. Bailey, R. Eustice, M. Jakuba, K.-i. Nakamura, C. Roman, T. Sato *et al.*, "Deep sea underwater robotic exploration in the ice-covered arctic ocean with auvs," in *2008 IEEE/RSJ International Conference on Intelligent Robots and Systems*. IEEE, 2008, pp. 3654–3660.

[10] E. Gallimore, M. Anderson, L. Freitag, and E. Terrill, "Synthetic baseline navigation using phase-coherent acoustic communication signals," *The Journal of the Acoustical Society of America*, vol. 146, no. 6, pp. 4831–4841, 2019.

[11] E. Gallimore, J. Partan, I. Vaughn, S. Singh, J. Shusta, and L. Freitag, "The whoi micromodem-2: A scalable system for acoustic communications and networking," in *OCEANS 2010 MTS/IEEE SEATTLE*. IEEE, 2010, pp. 1–7.

[12] T. E. Schneider and H. Schmidt, "Goby-acomms version 2: extensible marshalling, queuing, and link layer interfacing for acoustic telemetry," *IFAC Proceedings Volumes*, vol. 45, no. 27, pp. 331–335, 2012.

[13] T. Schneider, S. Petillo, H. Schmidt, and C. Murphy, "The dynamic compact control language version 3," in *OCEANS 2015-Genova*. IEEE, 2015, pp. 1–7.